PAPER Nr. : 9

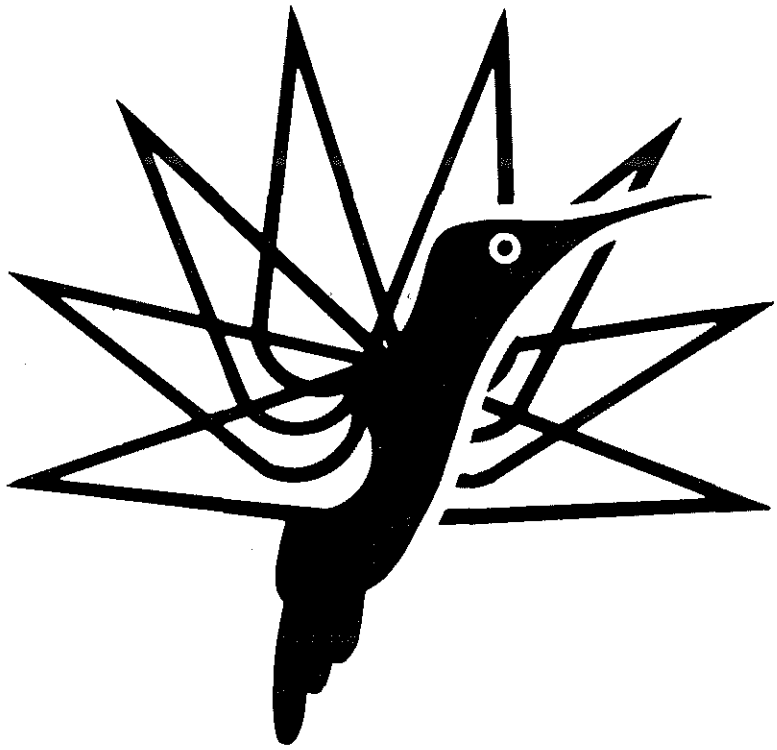

HIGH-SPEED DAUPHIN FUSELAGE AERODYNAMICS

BY

A. CLER

AEROSPATIALE HELICOPTER DIVISION
MARIGNANE, FRANCE

FIFTEENTH EUROPEAN ROTORCRAFT FORUM

SEPTEMBER 12 - 15, 1989 AMSTERDAM

ABSTRACT

This paper discusses the results of fuselage aerodynamics research by the Aérospatiale Helicopter Division since the early 1980s, leading to the advanced fuselage design of the High-Speed *Dauphin* or DGV*.

A rotor head fairing compatible with the Spheriflex rotor was initially designed on the basis of theoretical analysis using a panel method and a 3-dimensional boundary layer method. Preliminary wind tunnel tests on a simplified mockup showed the drag reduction that could be expected from a new aerodynamic concept in which the rotor head was completely integrated in the fuselage-cowling assembly. A final design was produced using the "CATIA" 3-dimensional CAD system, based on Turbomeca ARRIEL engines and a 5-blade Spheriflex rotor head 200 mm shorter than the Starflex rotor head used on the SA 365N. The design was slightly modified to take account of 3-dimensional calculations of the cowling pressure field.

The results of several years of research efforts on air intakes were used to design semistatic intakes fully integrated into the cowling profile for the ARRIEL engines. The redesigned air intakes and new engine exhaust nozzles provide excellent performance in high-speed flight, while maintaining suitable hover characteristics. A new MGB compartment ventilation system was developed after hydrodynamic tests and Navier-Stokes analysis by ONERA.

Wind tunnel testing of the final version showed a 20% reduction in drag compared with the already highly streamlined fuselage of the standard *Dauphin* and excellent handling qualities in high-speed flight.

CONTENTS

*DGV: *"Dauphin grande vitesse"*

1 - INTRODUCTION

The high-speed *Dauphin* (DGV*) is a prototype aircraft developed to test new technical solutions for implementation in a production aircraft during the next decade. Financed by the French aviation authorities, this research program comprises two major innovations:

- a new 5-blade Spheriflex rotor, more compact and 200 mm shorter than the previous Starflex rotor head;
- lower fuselage drag due to better integration of the rotor head in the upper cowlings.

By combining a streamlined fuselage and increased blade surface area, it will be possible to extend the airspeed envelope beyond the current reference (i.e. the 365N *Dauphin*) without requiring substantially higher engine power ratings. The objective is to increase the maximum airspeed by reducing the power requirement rather than by increasing the available power.

This paper discusses the work done in the area of fuselage aerodynamics at the Aérospatiale Helicopter Division since the early 1980s, leading to the highly streamlined DGV fuselage that has been undergoing flight tests since the spring of 1989.

2 - BASIC FUSELAGE DESIGN

The reference aircraft, the 365N *Dauphin*, has a highly streamlined fuselage and is one of the fastest helicopters of its generation. Any further drag reductions therefore represented an ambitious undertaking.

The idea behind the additional streamlining considered for the high-speed *Dauphin* is relatively simple to express, if not to implement. In many existing helicopters, notably the SA-365N, a streamlined fuselage is topped by a main rotor consisting of a rotor mast, pitch-control links and a rotor head designed with very little attention to aerodynamic considerations.

Wind tunnel tests of a relatively clean mockup of the standard *Dauphin* design (Figure 1) showed that the equivalent drag surface area (CxS) was 1.05 m^2, including 0.44 m^2 for the rotor head alone. Any further attempts to reduce fuselage drag without a corresponding reduction in rotor head drag would thus be illusory: the drag coefficient (Cx) of the *Dauphin* fuselage relative to its cross sectional area is about 0.1, compared to about 1.3 for the Starflex rotor head.

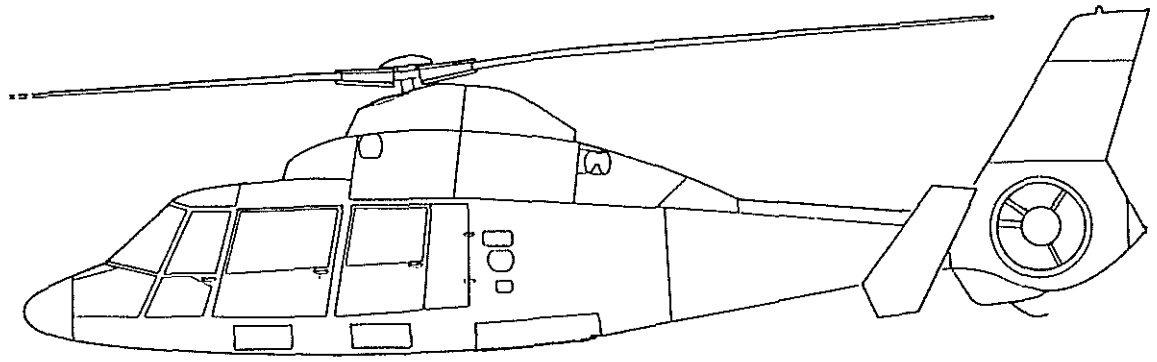

Figure 1 SA-365N *Dauphin* fuselage

*DGV: *"Dauphin grande vitesse"*

The main rotor geometry is dictated primarily by mechanical laws, with little latitude for aerodynamic criteria. The innovation in this design was to integrate the rotor head in a compact assembly comprising the fuselage together with the engine and MGB cowlings, and to add a lenticular rotor head fairing. The result (Figure 2) is a streamlined assembly with no remaining external transmission components: the helicopter thus achieves a condition long ensured for fixed-wing aircraft.

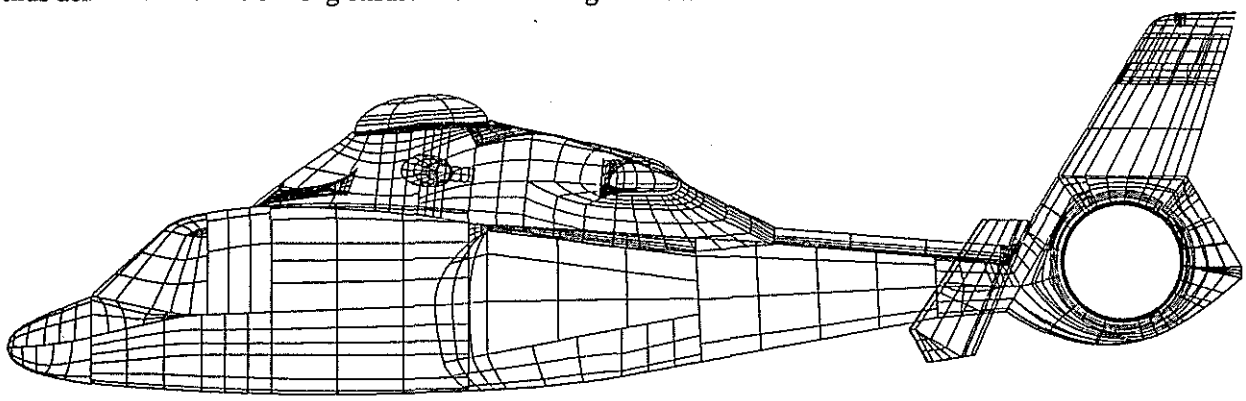

Figure 2 CATIA design of high-speed *Dauphin* fuselage

3 - ROTOR HEAD FAIRING DESIGN

A significant feature of the new 5-blade Spheriflex rotor head developed for the high-speed *Dauphin* is the short blade attach radius (550 mm, compared with 690 mm in the initial Starflex design). This is a major factor in reducing rotor drag: the lower CxS is due to the diminished frontal surface area S, not to a lower Cx coefficient.

The next step was to lower the Cx coefficient by adding a rotor head fairing. Research began in 1985 to define a "general design philosophy" for lenticular fairings. Two analysis tools were available at Marignane for this purpose:

- a conventional panel method using "source" type singularities;
- a 3-dimensional boundary layer method developed by ONERA/CERT and coupled with the panel method.

These programs were used to classify various lenticular fairing designs independently of the fuselage. Figure 3 shows a typical calculation in which the separation line was determined along the trailing portion of the fairing.

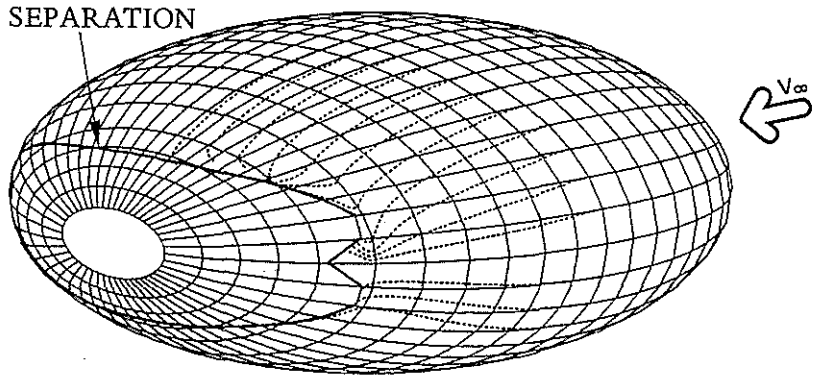

Figure 3 Calculated separation line on a lenticular fairing

Unfortunately, existing methods were unable to calculate either the wake downstream from the separation line or the drag; a simplified method was therefore used to estimate the drag from the position of the separation line. This approach would be particularly inaccurate if no distinction were made between large vortex-flow wakes and eddy-flow wakes.

For lenticular fairings, it can reasonably be assumed that boundary layer separation is not related to significant 3-dimensional effects, but simply to the longitudinal pressure gradient on the aft portion. The result is an eddy-flow wake characterized by a "dead water" region of relatively uniform pressure near the fairing.

Friction drag is negligible compared with pressure drag in the case of a thick fairing, and can be expressed as follows for a two-dimensional body of width L (Figure 4):

$$CxS = L \cdot \int_{o}^{ys} [Cp_i(y) - Cp_s]dy$$

where Cp_s is the pressure coefficient along the separation line determining the base pressure, and $Cp_i(y)$ is the "ideal" pressure coefficient calculated for an ideal (unseparated) fluid in the separation zone. This expression corresponds to the fact that there is no drag in an ideal inviscid fluid, and that pressure drag arises from the difference between the ideal pressure and the base pressure.

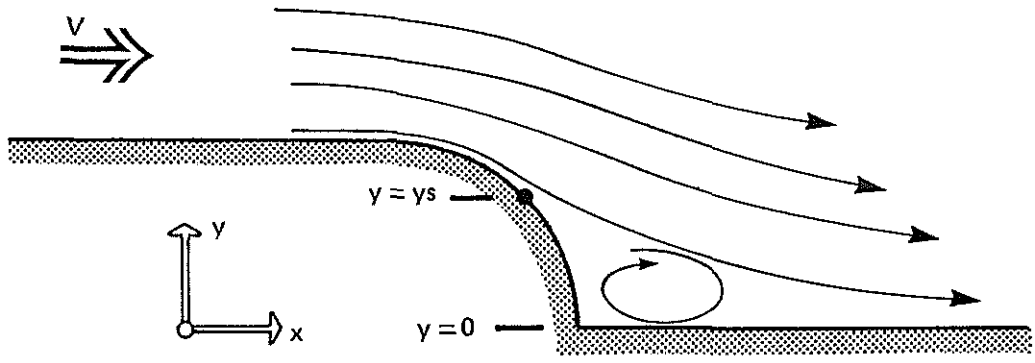

Figure 4 Schematic representation of airflow aft of separation on fairing

Potential flow calculations showed that on the symmetry plane of the lenticular fairings (corresponding to the fuselage symmetry plane) the $Cp_i(y)$ coefficient varied as a virtually linear function of y in the separation zone. The preceding relation is therefore easily integrated, giving the following formula:

$$CxS = (1-Cp_s) \cdot s/2$$

or

$$Cx = {}^1/_2(1-Cp_s) \cdot s/S$$

in which "s" is the separated frontal surface area, and "S" is the total frontal surface area of the fairing.

This reasoning is valid for two-dimensional flows. Similar integration for an axisymmetrical body such as a sphere gave the following relation:

$$Cx = {}^1/_3(1-Cp_s) \cdot s/S$$

Considering that the separated regions revealed by boundary layer calculations were nearly rectangular (when viewed looking upstream) the first formula was used to estimate the drag coefficient for various lenticular fairings. This relation cannot be expected to provide an accurate drag value since the pressure coefficient Cp_s given by ideal fluid calculations is necessarily inexact, but the approximate values based on physical criteria can be used to compare different shapes.

Figures 5 and 6 show the results obtained for fairings 250 mm high and 1000 or 1250 mm in diameter, assumed to be placed on a flat surface. In each figure the generatrices are an ellipse for shape 1, a 3rd-order super-ellipse for shape 2, a 1.5-order super ellipse for shape 3, and a circular arc for shape 4.

The ellipse provides a satisfactory compromise between the faired volume and the resulting drag coefficient, while the 3rd-order super-ellipse results not only in a larger frontal surface area S but also a higher drag coefficient Cx, and therefore in a significant increase in total drag.

The most pertinent result of this comparison is that the better streamlining of the shapes in Figure 6 due to the larger diameter did not lead to a lower drag (CxS) than for the shapes in Figure 5, since the gain in Cx was offset by an increase in S.

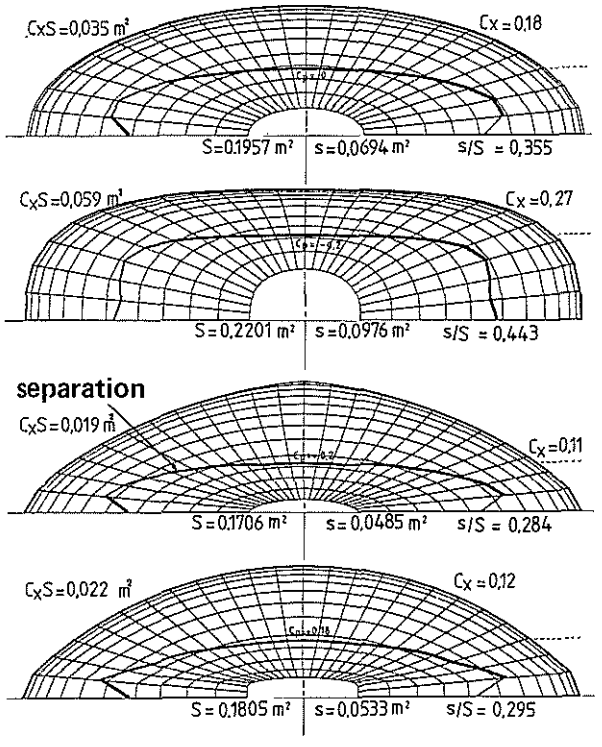

Diameter 1000 mm
Thickness 250 mm

Figure 5 Estimated drag for fairings 1000 mm in diameter and 250 mm thick

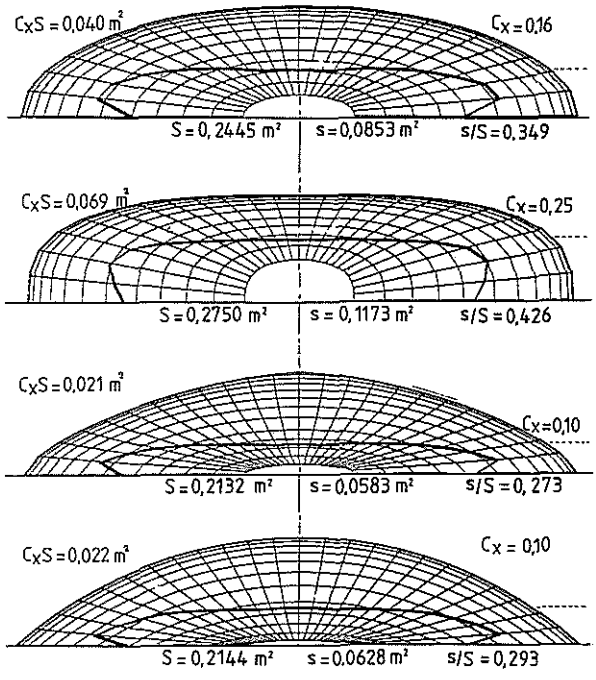

Diameter 1250 mm
Thickness 250 mm

Figure 6 Estimated drag for fairings 1250 mm in diameter and 250 mm thick

After analyzing these results, an ellipsoidal rotor head fairing with minimum clearance around the mechanical components was selected for the high-speed *Dauphin*. As shown in Figure 7, the blade attachment point at the tip of the sleeve was even allowed to protrude from the fairing to conserve a pure geometry and minimize the drag-inducing frontal area. The resulting shape is very near the ellipse in Figure 5. A 3rd-order super-ellipse would have been necessary to enclose the entire sleeve: this solution would virtually have doubled the total drag due to the fairing alone, and when installed on the fuselage it would have been poorly integrated with the overall cowling shapes, resulting in additional interaction drag.

A rotor head fairing would obviously penalize maintenance accessibility on a production aircraft. For a fairing integrated with the fuselage cowlings as on the DGV, an acceptable solution would be to design the fairing as an easily removable fairing secured to the rotor head at a few points like the hub caps installed on many existing helicopter rotors.

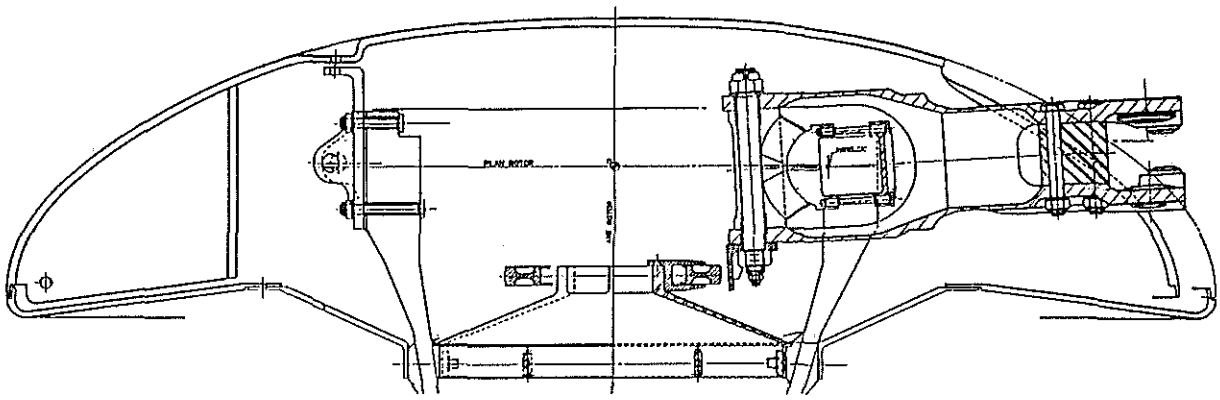

Figure 7 Fairing design for 5-blade Spheriflex rotor head on high-speed *Dauphin*

4 - AIRCRAFT COWLING DESIGN

The cross sectional area of the SA-365N cowlings has already been minimized, and further appreciable improvements in the drag coefficient for this portion of the fuselage were unlikely. Nevertheless, the cowling design had to be modified to ensure suitable integration of the rotor head fairing and to accommodate the wider mechanical power transmission assembly.

Figure 8 compares the rotor transmission systems for the SA-365N and the DGV. The rotor head height reduction in the new version resulted in a larger diameter carbon mast and pitch-change link assembly, requiring wider fairings: Figure 9 compares the frontal aerodynamic analysis mesh for the two aircraft (the 365N is shown without the rotor head).

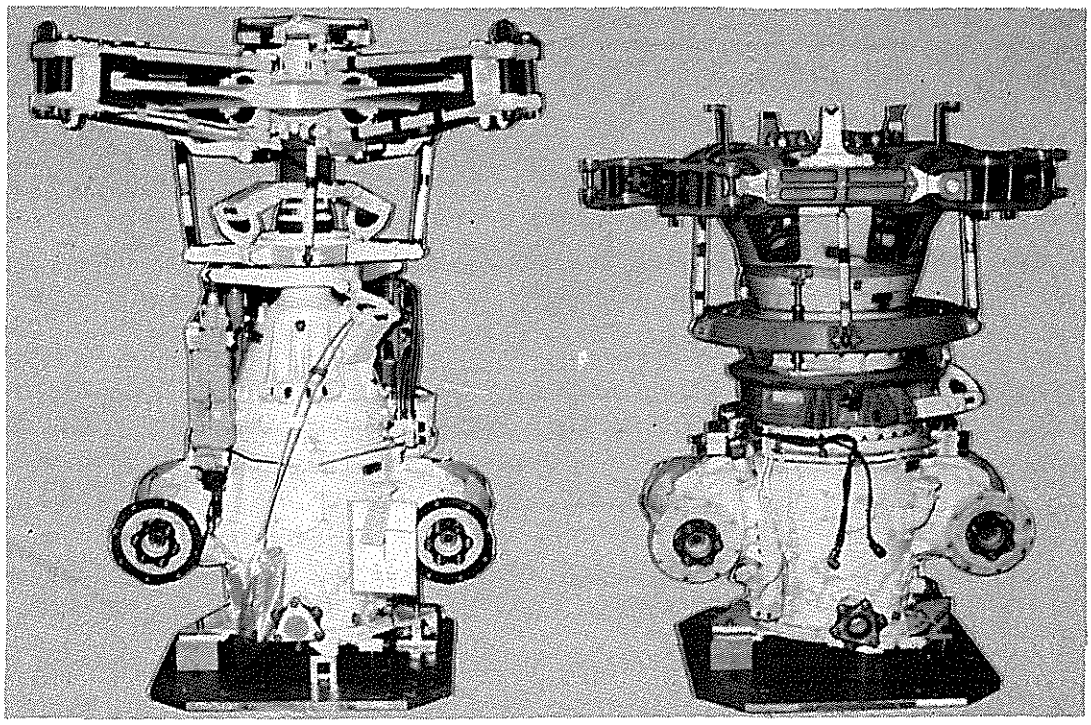

Figure 8 Rotor transmission components on SA-365N and DGV

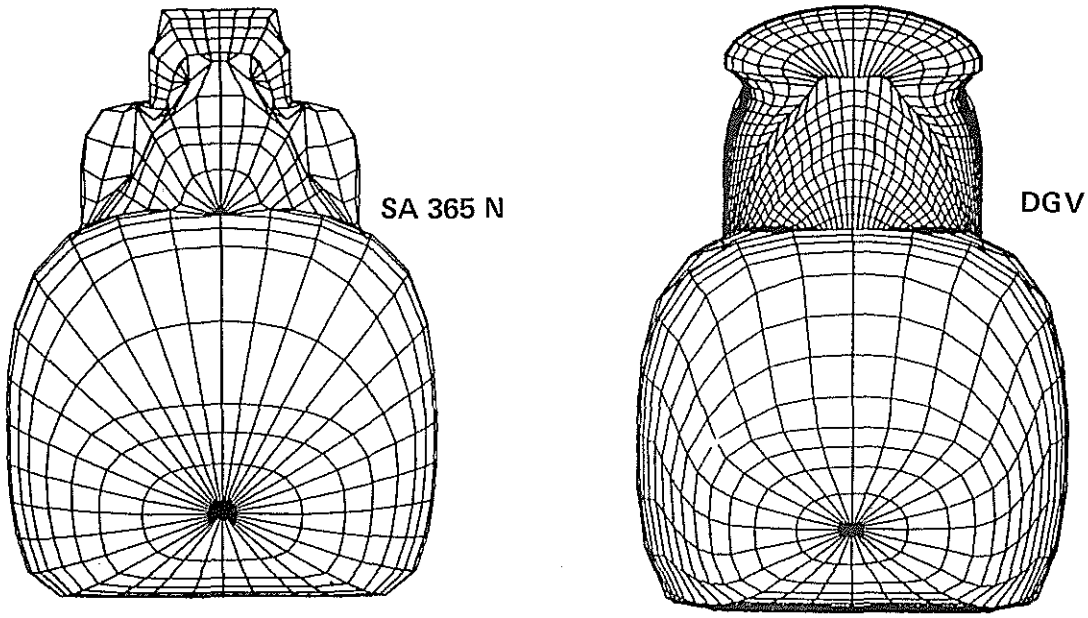

Figure 9 Frontal surface area of standard *Dauphin* and DGV (without rotor head on SA-365N)

An initial simplified cowling design was generated in 1986 using a 2-D CADAM system. This was immediately followed by wind tunnel testing of various engine cowling geometries with both 4- and 5-blade rotor heads to assess the aerodynamic properties of this type of fuselage. At that time the number of blades and the powerplant (Turboméca ARRIEL or TM 333) had not been finalized.

Figure 10 shows a wind tunnel test mockup with idealized exhaust nozzle contours, and Figure 11 a more realistic CADAM rendering of the cowling design for the ARRIEL engines.

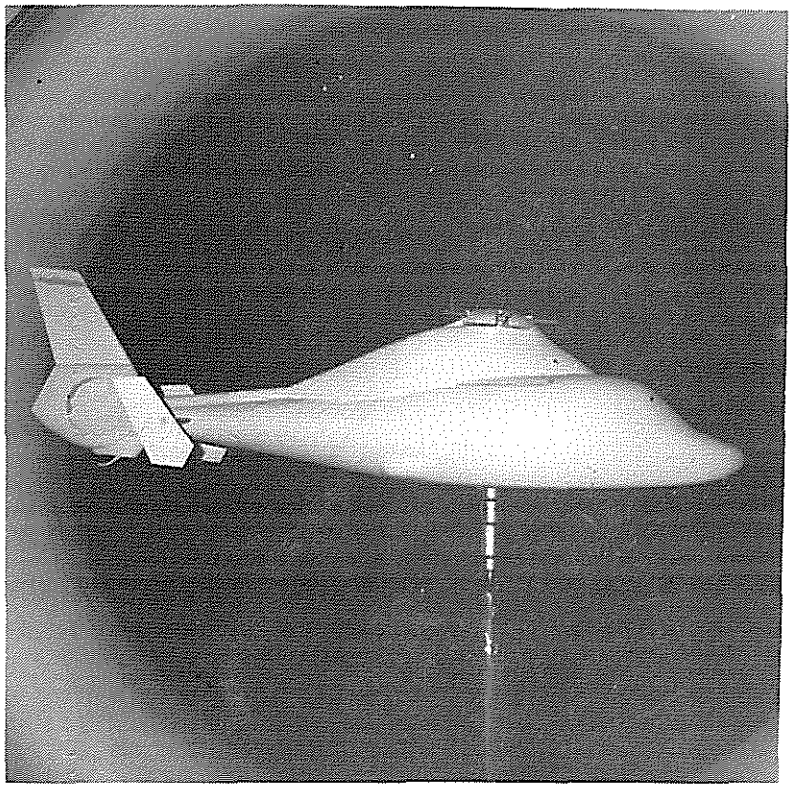

Figure 10 Initial high-speed *Dauphin* mockup in Marignane wind tunnel

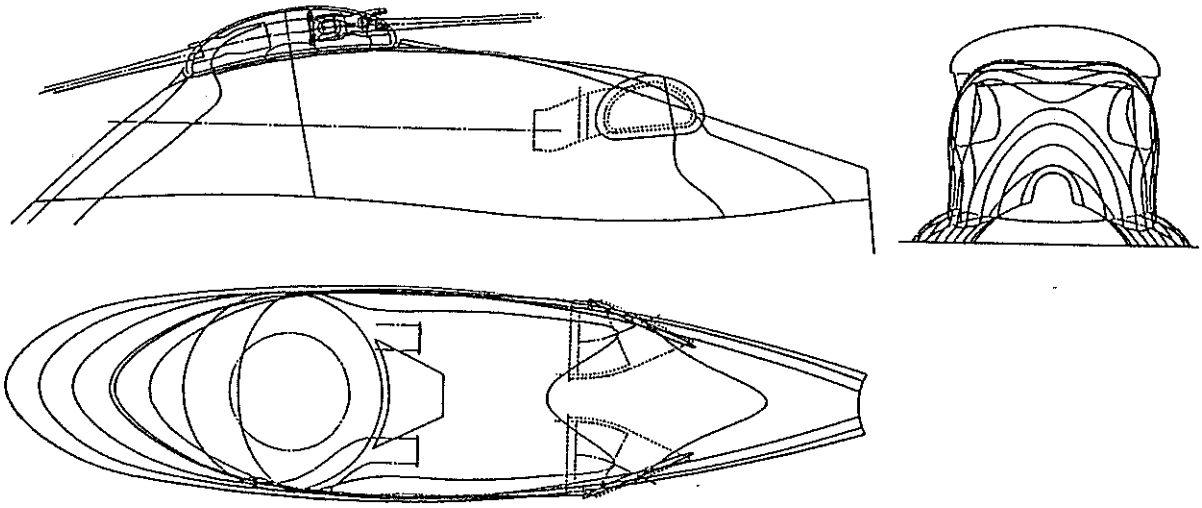

Figure 11 Preliminary high-speed *Dauphin* cowling design

The final cowling design (Figure 2) was produced in 1987 using the "CATIA" 3-D CADAM system and based on the final design options:

- 5-blade Spheriflex rotor head
- two ARRIEL 1C1 or ARRIEL 1X* engines

The transition from four to five blades obviously involved a drag penalty due to the greater number of openings in the rotor fairing, but was dictated by two imperatives for the high-speed *Dauphin*:

- a greater blade surface area is necessary at high speeds using the original *Dauphin* rotor blades;
- a very low vibration level equivalent to the production SA-365N must be maintained at significantly higher speeds (the speed increase and squat rotor design of the DGV are both liable to increase vibration levels with the same number of blades).

The first wind tunnel tests showed that the change from 4 to 5 blades had only a minor effect on drag (the increase in CxS was only about 0.03 m^2).

When the CATIA design was available it was then possible to construct an aerodynamic mesh (Figure 12) for the panel method. The objective was mainly to determine the pressure field around the cowling in order to optimize the engine air intake and ventilation inlet/outlet positions.

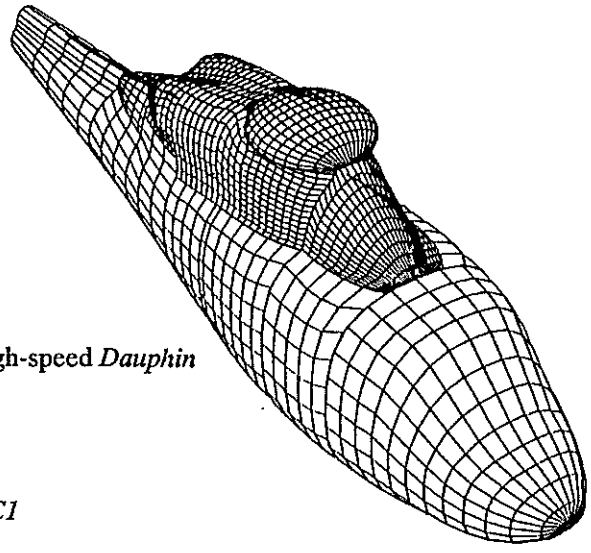

Figure 12 Fuselage aerodynamic mesh for high-speed *Dauphin*

**a higher-power prototype derived from the ARRIEL 1C1*

The mesh was also used to streamline the design, as the initial calculations showed that intense negative pressure zones with a pressure coefficient (Cp) of about -1 existed around the rotor fairing. Because recompression of the airflow occurred downstream from these depressions, and since this type of recompression favors boundary layer separation, it was considered that drag could be reduced by minimizing the extent of the low pressure region.

This was done in three iterations by modifying the shape of the cowlings in the zone next to the rotor fairing. Figure 13 shows the original design and the improved version, with a narrower cross section beneath the rotor head fairing. The idea was to maintain equivalent surface areas by reducing the cross sectional area of the cowlings to offset the increased area of the rotor head fairing.

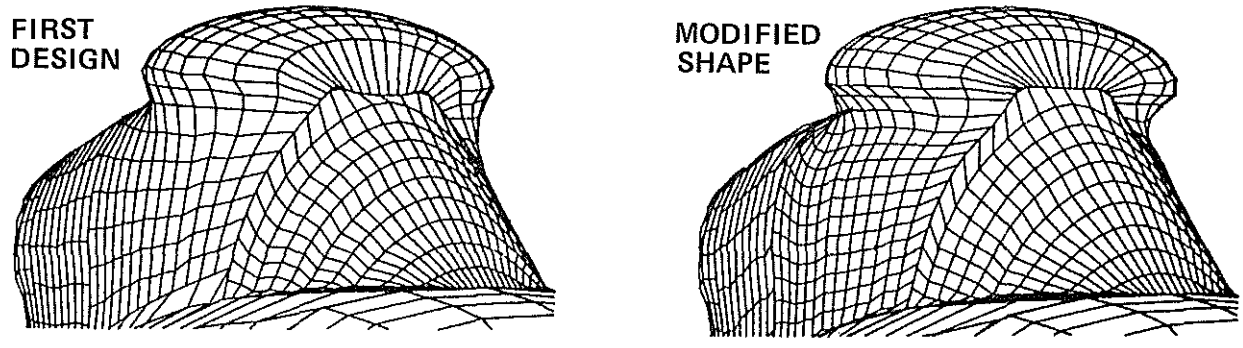

Figure 13 Improved transition from cowling to rotor head fairing after aerodynamic analysis

An attempt was then made to use the 3-dimensional boundary layer method available at Marignane. Little information was expected from this analysis, since wind tunnel tests had shown that separation occurred neither on the fuselage nor on the cowlings except immediately downstream from the rotor head. Moreover, boundary layer calculations are more difficult with complex shapes such as the high-speed *Dauphin* fuselage than with more stylized shapes such as the ellipsoid in Figure 3.

A typical result is shown in Figure 14, where the wall flow lines (skin friction lines) are shown along a fuselage at zero incidence angle. Boundary layer calculations confirmed that separation did not occur along the cowling sides except downstream from the rotor head and immediately aft of the exhaust outlets. (We shall see in a moment that the exhaust nozzles were redesigned after this calculation).

Figure 14 also shows that the lateral engine air intakes beneath the rotor head are relatively well protected in falling rain from ingress of water flowing aft along the fuselage.

The boundary layer analysis provided further useful information for redefining the engine bay ventilation system. Even with a perfectly smooth outer surface the boundary layer over the engine cowlings is about 30 mm thick (corresponding to a 4 mm displacement thickness) and allowance must be made for this fact in designing the engine bay ventilation air inlets.

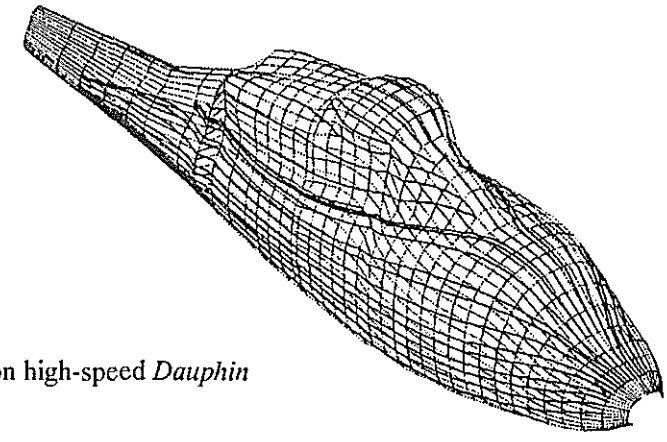

Figure 14 Calculated skin-friction lines on high-speed *Dauphin* fuselage at 0° incidence

5 - ENGINE AIR INTAKE DESIGN

The wider rotor transmission system made it more difficult to install Pitot type dynamic air intakes on the DGV than on the SA-365N. This was not a serious problem, however, as research programs since 1982 have allowed Aérospatiale to acquire considerable experience with another design: static air intakes.

Wind tunnel tests and flight tests on the AS-355 TwinStar have shown that excellent performance can be obtained with static air intakes integrated in the shape of the cowlings: the lower pressure recovery is offset by much lower drag. Figure 15 compares pressure recovery on a 1:2 scale wind tunnel mockup of the TwinStar for a conventional dynamic air intake and a purely static air intake with a suitably rounded forward lip. Both air intakes supply an engine with an air intake scroll (Turboméca TM 319). It may be seen that, despite its name, the "static" air intake allows appreciable dynamic pressure recovery that increases with the airspeed.

The engine and MGB layout on the high-speed *Dauphin* allowed "semistatic" air intakes to be fully integrated into the cowling wall, with an intermediate geometry between the two extremes mentioned above. Their shape ensures pressure recovery between the two curves in Figure 15.

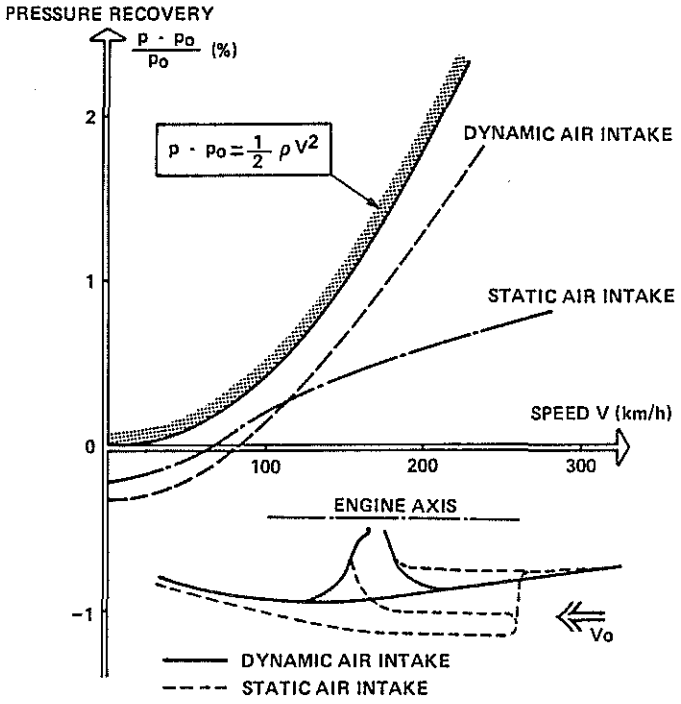

Figure 15 Comparative pressure recovery with static and dynamic air intakes

Another advantage of this design is greater protection against ingestion of foreign objects (e.g. birds) during high-speed flight. For complete safety, Aérospatiale screens all air intakes with 0.8 mm diameter wire on a 5.5 mm mesh. The pressure drop due to a screen in the airstream depends primarily on the solidity of the screen. When the wires are widely spaced, losses are attributable to the drag of each wire considered alone (this drag is not negligible, given the low Reynolds numbers involved). As the mesh is tightened, unfavorable interactions appear among the wires and the pressure drop increases.

Figure 16 (excerpted from Hoerner) plots the pressure drop versus the screen solidity. With a solidity factor of 0.25 as used by Aérospatiale, Hoerner reports a drop of about 40% of the upstream dynamic pressure. Tests at Marignane directly on aircraft protection screens showed a somewhat lower pressure drop of about 30%. These values refer to screens placed at right angles to the airstream. With a static or

semistatic air intake, the screen is more tangent to the air flow and the pressure drop problem must be reconsidered. A study was conducted in 1984 to assess the effects of tangential incidence on the pressure drop. Wind tunnel tests showed that the pressure drop was unaffected by incidence angles between 90° and 30°, while at lower angles the screen permeability diminished and the pressure drop increased (Figure 17).

The DGV air intake screens were therefore designed to prevent the airstream from striking the mesh at an angle below 30° in high-speed flight.

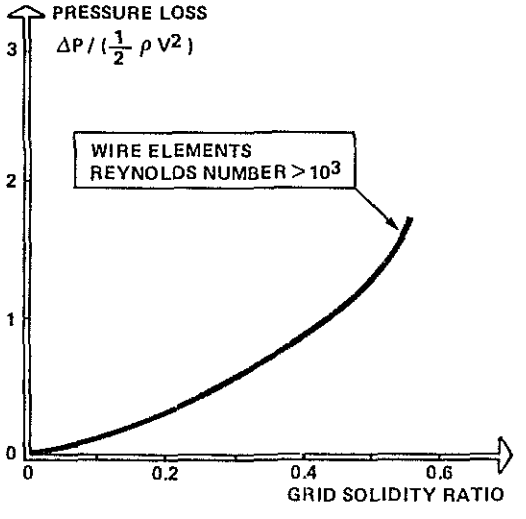

Figure 16 Pressure drop across a screen at right angles to the airstream versus mesh solidity factor

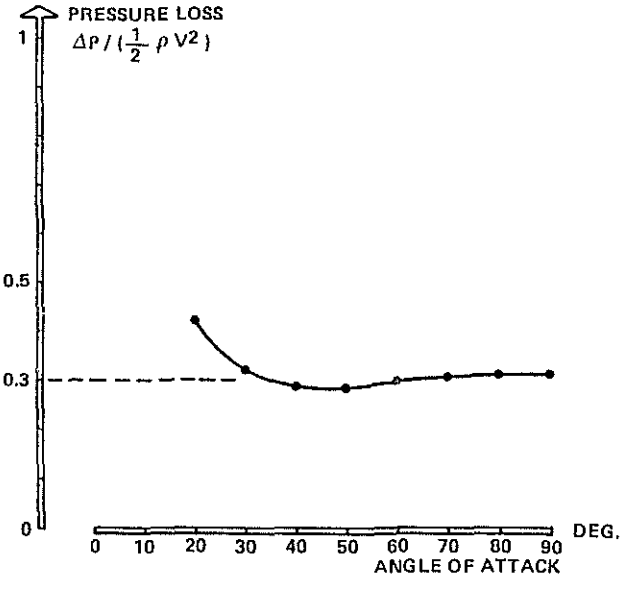

Figure 17 Air intake screen pressure drop versus incidence angle

6 - ENGINE EXHAUST NOZZLES

In optimizing an aircraft for high-speed flight it is tempting to design the exhaust nozzles with a small cross section to recover some residual thrust from the increased engine exhaust gas velocity. However, the high-speed *Dauphin* is an experimental platform for technical solutions applicable to future production aircraft, and hover performance cannot be disregarded. The exhaust nozzle cross section was therefore unchanged from the standard SA-365N. The exhaust gas stream is also used to provide suction effect for ventilating the engine bays.

A major design parameter was the angle between the exhaust jet axis and the aircraft centerline. An axial exhaust stream obviously enhances the recovered jet momentum, but can lead to dangerous overheating of the tail boom when the exhaust stream is swept down onto the structure by the rotor blast in hover. The composite material constituting the *Dauphin* tail boom is relatively sensitive to overheating, and a 25° lateral exhaust angle was selected for the initial design in 1986. Considering that cos(25°) 0.9, this angle continued to provide satisfactory use of exhaust momentum in forward flight. At the final design stage in 1987, the 25° elbow in the exhaust ducts was found to be incompatible with the overall cowling design, resulting in an external flow separation zone immediately downstream from the outlet. The angle was therefore reduced to 20°, which has proved to be a satisfactory tradeoff between drag and overheating problems.

7 - MAIN GEARBOX VENTILATION

The MGB ventilation air intake on the DGV was located near its position on the SA-365N, i.e. at the forward end of the MGB cowling where it benefits from natural flow compression in high-speed flight. The outlet had to be relocated, however, as the rotor head fairing prevented the use of a "chimney" around the rotor mast as on the SA-365N. The outlet was therefore located immediately aft of the rotor head fairing as shown in Figure 18. The airstream is ejected as nearly horizontal as possible through a duct that was not excessively necked down in order to ensure satisfactory ventilation in hovering flight. Figure 19 is a closeup view of the ventilation system outlet.

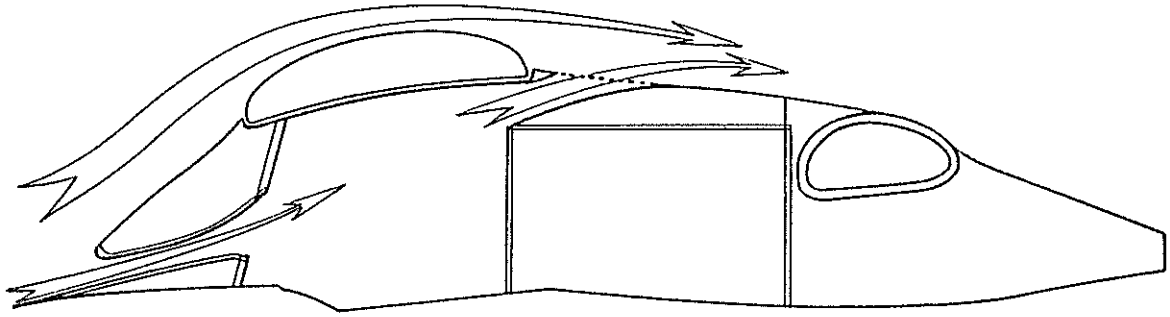

Figure 18 Schematic view of MGB compartment ventilation system

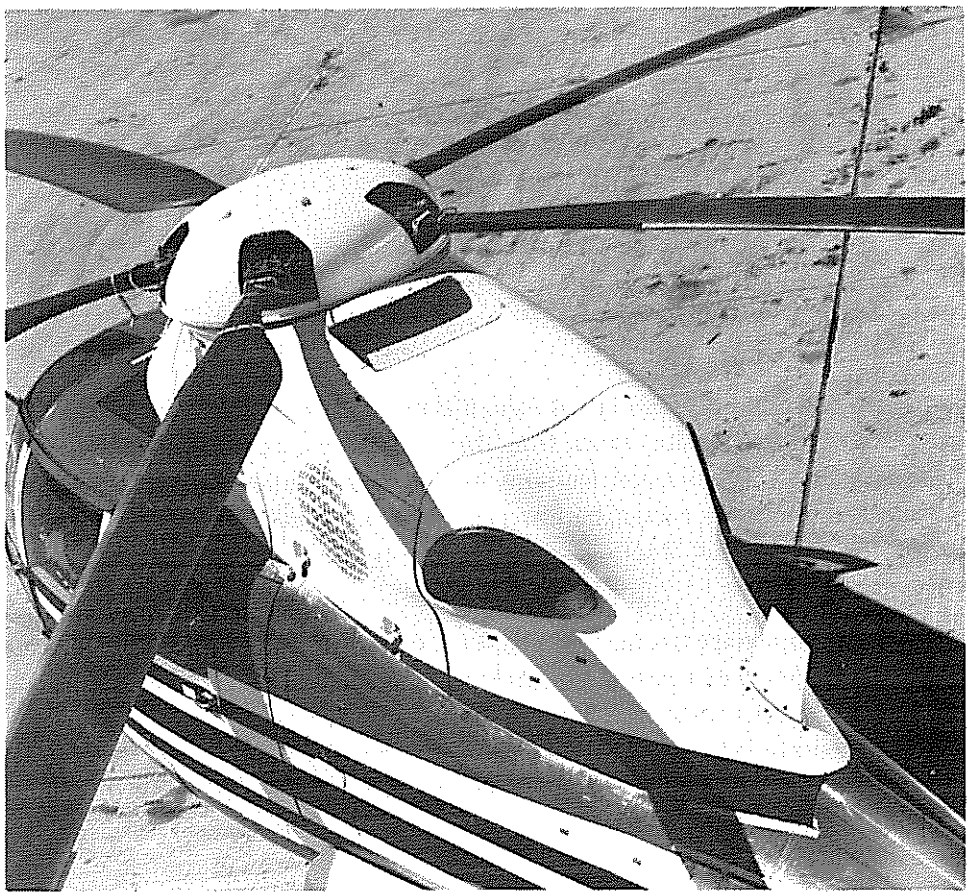

Figure 19 View of MGB compartment ventilation outlet on aircraft

The MGB ventilation airflow has far from negligible effects on the external fuselage aerodynamics, representing some 1.5 $kg \cdot s^{-1}$ compared with 3 $kg \cdot s^{-1}$ for the engine exhaust. The question was whether this airstream could be used to improve the airflow characteristics around the cowling and rotor head fairing assembly.

A preliminary experiment was conducted in the ONERA hydrodynamic tunnel at Chatillon using a stylized mockup of a rotor head fairing mounted on the cowlings. Longitudinal ventilation outflow was simulated at various flow velocities from a slot at the back of the lenticular fairing. Dyes and air bubbles were added to the stream to visualize the flow around the mockup. Figure 20, for example, shows the effect of an outflow velocity equal to 3 times the exterior air flow velocity (V_∞). The tests showed that the outflow conditions for the high-speed *Dauphin* (i.e. between $\frac{1}{2}V_\infty$ and V_∞) had no appreciable effect on the downstream wake compared with the conditions prevailing without any ventilation outflow. A very strong but unrealistic ejection stream (approx $3V_\infty$) was required to reduce the rotor head wake volume.

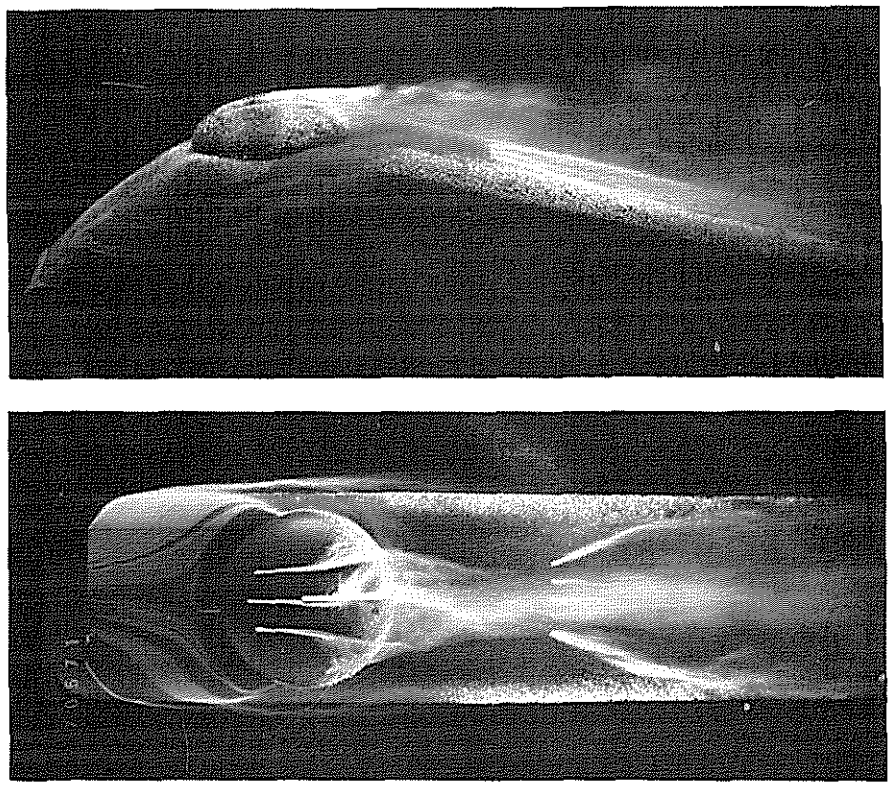

Figure 20 Ventilation exhaust tests in ONERA hydrodynamic test facility

The tests were performed at very low Reynolds numbers not representative of actual flight conditions, and this result had to be considered subject to caution. A second approximation was therefore attempted using a 2-D Navier-Stokes analysis program available at ONERA/CERT. The CERT had investigated the effect of a tangential outflow jet at the base of a recirculation pocket behind a descending step. This geometry corresponded very schematically to the problem of flow separation aft of the rotor head fairing. Figure 21 is an example of the effect of an outflow jet at $\frac{1}{2}V_\infty$ and at V_∞ on the flow structure. Analysis of the downstream momentum values corroborated the hydrodynamic test results: at moderate velocities the outflow jet does not appreciably alter the downstream wake structure.

Following these two studies, it was considered that the position selected for the MGB compartment ventilation outflow port did not improve the external airflow patterns, but at least did not impair them as might have been the case with a more transversal outlet position.

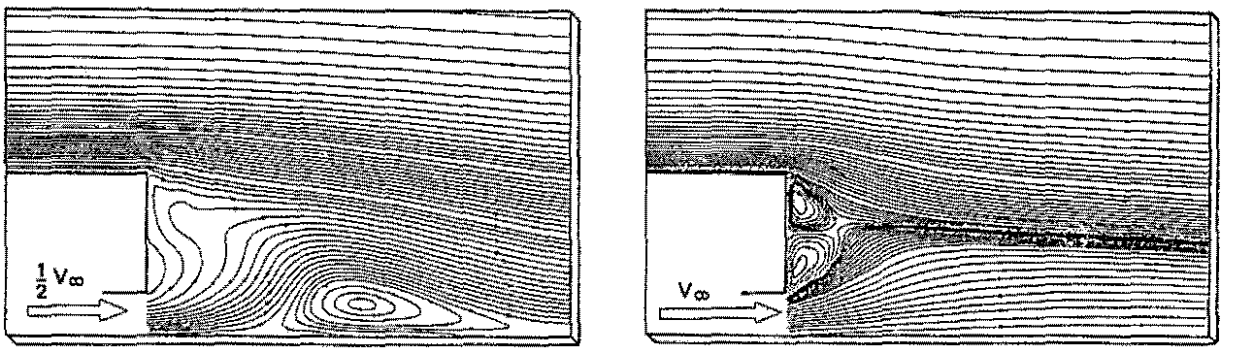

Figure 21 Navier-Stokes calculation of ventilation exhaust effect in flow-separated region by ONERA/CERT (flow line plots)

8 – WIND TUNNEL TEST RESULTS

The final DGV fuselage design was tested as a 1:7.7 scale model and compared with an SA-365N reference model in the Marignane wind tunnel (Figure 22).

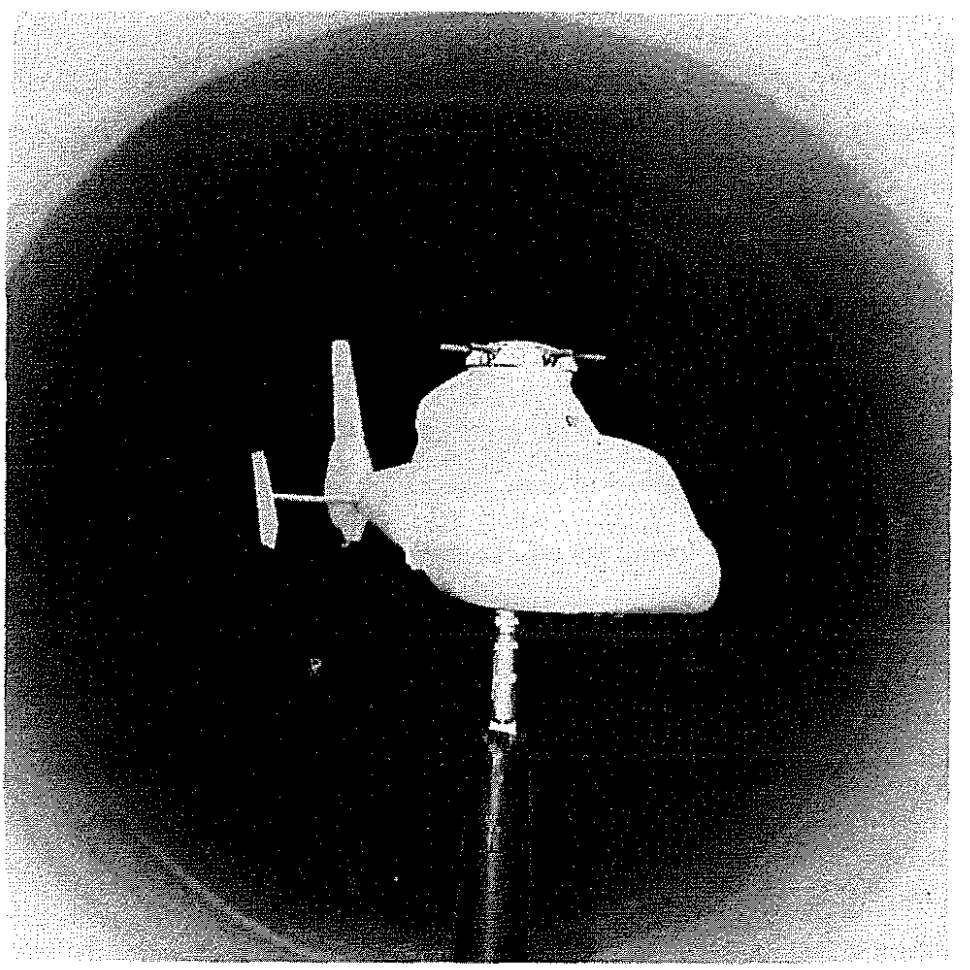

Figure 22 Final high-speed *Dauphin* mockup in Marignane wind tunnel

The models are relatively clean, and do not simulate internal airflows, so no precise drag predictions can be made on the basis of the results. The primary objective was to estimate the difference in drag compared with a reference model corresponding to a well known aircraft. The following results were obtained at 0° incidence:

Standard 365N	CxS = 1.05 m^2
DGV with rotor fairing	CxS = 0.85 m^2
DGV w/o rotor fairing	CxS = 0.92 m^2

It should be noted that the roughly 20% drag reduction observed on the high-speed *Dauphin* complete with its rotor head fairing, due in large part to the redesigned rotor head, significantly modifies the relative components in the total aircraft drag, as shown in the following table:

Aircraft	Rotor head	Fuselage + cowlings	Tail unit: horiz. stabilizer, tail fin, outboard fin & fenestron
SA-365N	42%	39%	19%
DGV	28%	48%	24%

On a highly streamlined helicopter such as the DGV, the rotor head is no longer the primary source of drag. Future streamlining work can be devoted to the fuselage surface finish and to balance-related drag. This is the reason the high-speed *Dauphin* will be fitted in 1990 with a tail fin flap adjustable in flight to minimize yaw balancing drag for each flight configuration (i.e. irrespective of the aircraft weight, airspeed and altitude).

One beneficial consequence of the reduced drag is the improved airflow around the tail unit, notably the tail fin. The fuselage yawing moment is expressed as a dimensionless Cn coefficient (obtained by dividing the actual moment by the dynamic pressure in flight $\frac{1}{2}\rho V^2$ and by the reference volume πR^3 based on the main rotor radius R). At zero incidence and sideslip:

Standard 365N	$100 \cdot Cn = 0.71$
DGV with rotor fairing	$100 \cdot Cn = 0.79$
DGV w/o rotor fairing	$100 \cdot Cn = 0.74$

The airstream striking the tail fin is thus improved on the high-speed *Dauphin* with its rotor fairing, and should allow the tail fin to fulfill its anti-torque function with a constant setting at airspeeds up to about 200 knots without requiring any tail rotor thrust action. (The existing 365N fin ensures the total anti-torque function at about 150 knots).

Figure 23 shows the yaw moment variation versus the sideslip angle (β) for the SA-365N and the DGV. The $Cn = f(\beta)$ curve for the standard 365N shows a characteristic notch at low sideslip angles when

the tail fin passes through the Starflex rotor wake; this notch is not observed with the DGV. At zero sideslip the results are the following:

$$d(100 \cdot Cn)/d\beta = 0.047/° \text{ for the 365N}$$
$$d(100 \cdot Cn)/d\beta = 0.078/° \text{ for the DGV}$$

i.e. a 65% increase in the weather-vane effect for the new design: this should result in excellent transversal dynamic stability at high speeds.

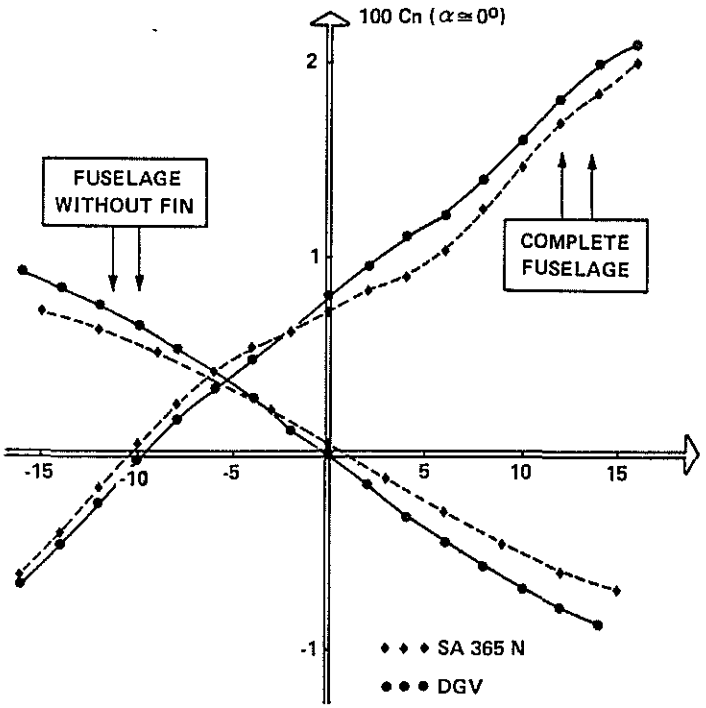

Figure 23 Yaw moment measured in wind tunnel on SA-365N and DGV fuselages

9 - RECENT ADVANCES IN MAIN ROTOR HEAD DESIGN

As mentioned earlier, the task of the aerodynamics engineer is primarily concerned with enclosing power transmission systems over which he has only a very limited influence. In this regard, he must adapt to technological changes often dictated by considerations other than aerodynamics, and notably rotor dynamics.

A new rotor head concept was advanced in 1988, and experimented on a modified SA-365N Starflex rotor head: the interblade damper system. The "interblade" concept uses viscoelastic adapters mounted between the blade sleeves. On the high-speed *Dauphin* with its 5-blade Spheriflex rotor head, it ensures greater simplicity and dynamic efficiency than a conventional design with hydroelastic dampers between the sleeve and rotor head. Both designs are shown in Figure 24.

Priority has therefore been given to providing the high-speed *Dauphin* with interblade adapters. This, however, raises a problem: at high flapping angles the adapter, which is located at some distance from the rotor centerline, rises beyond the limits of the volume defined for the rotor head fairing.

A new fairing had to be designed with less than optimum drag characteristics. Raising the fairing by 50 mm increases both the frontal surface area S and the drag coefficient Cx, so the final drag reduction is negligible in comparison with the unfaired rotor. Nevertheless, the new fairing continues to act as a rotor wake deflector (similar to a conventional hub cap), and was installed on the aircraft during the initial test flights in the spring of 1989 (Figures 25 and 26).

With the interblade adapters, the drag characteristics of the high-speed *Dauphin* are therefore practically the same as for the aircraft with an unfaired main rotor head (CxS = 0.92 m^2).

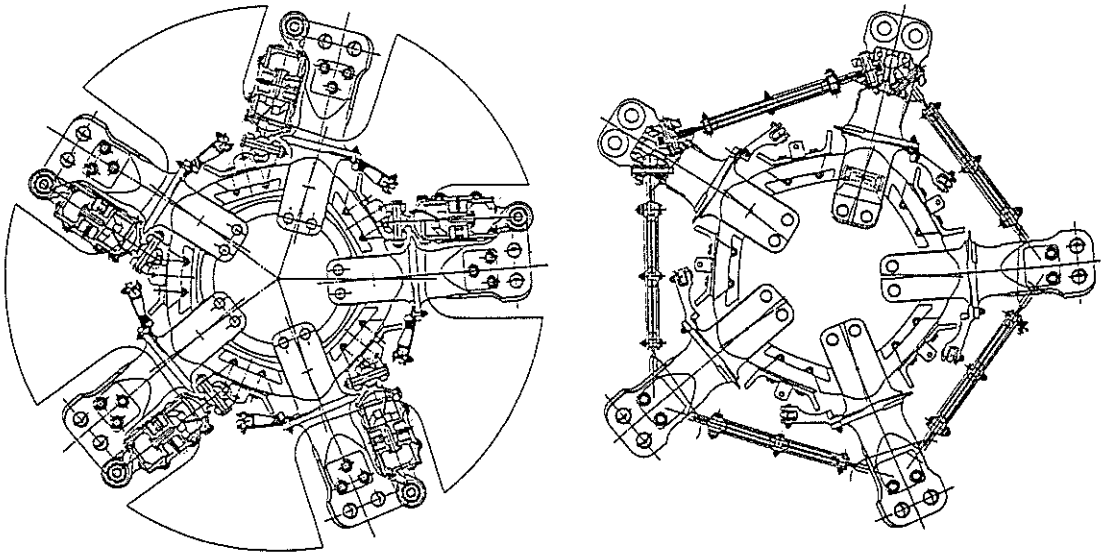

Figure 24 5-blade Spheriflex rotor head with conventional dampers and viscoelastic interblade dampers

Figure 25 High-speed *Dauphin* on the ground

Figure 26 High-speed *Dauphin* in flight

10 - CONCLUSION

The high-speed *Dauphin* (DGV) represents a breakthrough in fuselage aerodynamics: a rotor head fully integrated in the fuselage-cowlings assembly constituting a completely faired system with respect to external airflow.

This new concept was made possible by replacing the standard SA-365N rotor head with a shorter and more compact Spheriflex rotor head.

The DGV fuselage design is the outgrowth of an extensive research program in aerodynamics undertaken in the early 1980s under the auspices of the French aviation authorities.

Analytical methods and wind tunnel tests were used to optimize the rotor head fairing, the general shape of the highly streamlined upper cowlings, the semistatic engine air intakes, new engine exhaust ducts and a specially designed MGB compartment ventilation system.

Together, these modifications have resulted in a 20% drag reduction compared with the standard SA-365N *Dauphin*, already considered a highly streamlined aircraft.

This drag reduction, in conjunction with a new 5-blade main rotor should initially allow the *Dauphin* airspeed envelope to be extended by diminishing the aircraft power requirement.

Subsequently, beginning in 1990, new and more powerful engines and an upgraded main gearbox should allow the high-speed *Dauphin* to reach cruising speeds on the order of 200 knots.